Enhancer Turnover Is Associated with a Divergent Transcriptional Response to Glucocorticoid in Mouse and Human Macrophages

The Journal of Immunology

Enhancer Turnover Is Associated with a Divergent Transcriptional Response to Glucocorticoid in Mouse and Human Macrophages

Alasdair W. Jubb, Robert S. Young, David A. Hume and Wendy A. Bickmore

J Immunol 2016; 196:813-822; Prepublished online 9 December 2015;
doi: 10.4049/jimmunol.1502009
http://www.jimmunol.org/content/196/2/813

The Journal of Immunology is published twice each month by
The American Association of Immunologists, Inc.,
9650 Rockville Pike, Bethesda, MD 20814-3994.

Print ISSN: 0022-1767 Online ISSN: 1550-6606.

Enhancer Turnover Is Associated with a Divergent Transcriptional Response to Glucocorticoid in Mouse and Human Macrophages

Alasdair W. Jubb,*,†,[1] Robert S. Young,*,[1] David A. Hume,† and Wendy A. Bickmore*

Phenotypic differences between individuals and species are controlled in part through differences in expression of a relatively conserved set of genes. Genes expressed in the immune system are subject to especially powerful selection. We have investigated the evolution of both gene expression and candidate enhancers in human and mouse macrophages exposed to glucocorticoid (GC), a regulator of innate immunity and an important therapeutic agent. Our analyses revealed a very limited overlap in the repertoire of genes responsive to GC in human and mouse macrophages. Peaks of inducible binding of the GC receptor (GR) detected by chromatin immunoprecipitation-Seq correlated with induction, but not repression, of target genes in both species, occurred at distal regulatory sites not promoters, and were strongly enriched for the consensus GR-binding motif. Turnover of GR binding between mice and humans was associated with gain and loss of the motif. There was no detectable signal of positive selection at species-specific GR binding sites, but clear evidence of purifying selection at the small number of conserved sites. We conclude that enhancer divergence underlies the difference in transcriptional activation after GC treatment between mouse and human macrophages. Only the shared inducible loci show evidence of selection, and therefore these loci may be important for the subset of responses to GC that is shared between species. ***The Journal of Immunology*****, 2016, 196: 813–822.**

The gene complements of different mammals are remarkably similar (1), which implies that phenotypic variation is driven mainly by differences in transcriptional regulation (2–4). Expression of orthologous genes can differ between closely related primates (5) and even between individuals within a species (6), with genes involved in extracellular processes and the immune response being the most divergent (7). The most highly conserved and highly inducible promoters are, paradoxically, the most sensitive to variation in expression across species (8). Much of this divergence is driven by the evolution of *cis*-regulatory elements (9), such as enhancers (10).

Deep evolutionary conservation has been used to identify candidate enhancers (11, 12). Nevertheless, complete gain and loss of enhancers between species are also common (13–15). In mammals, at least, turnover of *cis*-regulatory elements can occur rapidly enough to be identified between strains of a single species (16). Most evolutionarily labile enhancers can be aligned to the genomes of distantly related species (17), suggesting that the acquisition of novel enhancers can occur through mobilization of existing sequences, including transposable elements (18). Species-specific regulatory elements display a level of nucleotide diversity consistent with a relaxation in evolutionary constraint (14). Because not all transcription factor binding sites have a direct effect on gene expression (18–20), these sites may represent functionally neutral sequence.

The profound differences in the immune systems of mice and humans have long been recognized (8, 21–23), and are accompanied by both high levels of gene expression divergence and *cis*-regulatory element turnover (7). This divergence is most likely driven by the evolutionary pressure of host–pathogen interactions, alongside changes in the expressed protein-coding sequences driven by positive natural selection (24).

Glucocorticoids (GC) are powerful metabolic hormones that are released in response to stress (25) and that provide natural feedback regulation of immune function. Exogenous GC are widely used as anti-inflammatory therapy (26). Accordingly, their actions on immune cells are likely to be affected by evolutionary selection. GC act by binding to an intracellular nuclear hormone receptor—the GC receptor (GR). Nuclear GR may bind directly to DNA, classically as a homodimer (27), to a canonical glucocorticoid response element (GRE), or may act indirectly by binding other transcription factors such as NF-κB and AP-1 (28), as well as by recruiting coregulators, for example, GRIP1 (29). Gene repression by GC in inflammation has been linked to binding of

*Medical Research Council Human Genetics Unit, Institute of Genetics and Molecular Medicine, University of Edinburgh, Edinburgh EH4 2XU, United Kingdom; and †Roslin Institute and Royal (Dick) School of Veterinary Studies, University of Edinburgh, Edinburgh EH25 9RG, United Kingdom

[1]A.W.J. and R.S.Y. contributed equally to this work.

ORCIDs: 0000-0001-5593-866X (A.W.J.); 0000-0002-8300-8002 (R.S.Y.); 0000-0001-6660-7735 (W.A.B.).

Received for publication September 11, 2015. Accepted for publication November 4, 2015.

A.W.J. is supported by Wellcome Trust Clinical PhD Fellowship 097481/Z/11/Z. W.A.B. and R.S.Y. are supported by unit program grants from the U.K. Medical Research Council (U.K.). The Roslin Institute is supported by Institute Strategic Programme Grants from the Biotechnology and Biological Sciences Research Council.

The microarray data and sequences presented in this article have been submitted to the National Center for Biotechnology Information Gene Expression Omnibus (http://www.ncbi.nlm.nih.gov/geo/) under accession number GSE61881.

Address correspondence and reprint requests to Prof. Wendy A. Bickmore or Prof. David A. Hume, Medical Research Council Human Genetics Unit, Institute of Genetics and Molecular Medicine, University of Edinburgh, Western General Hospital, Crewe Road, Edinburgh EH4 2XU, U.K. (W.A.B.) or Roslin Institute and Royal (Dick) School of Veterinary Studies, Easter Bush, Midlothian EH25 9RG, U.K. (D.A.H.). E-mail addresses: wendy.bickmore@igmm.ed.ac.uk (W.A.B.) or david.hume@roslin.ed.ac.uk (D.A.H.)

The online version of this article contains supplemental material.

Abbreviations used in this article: ChIP, chromatin immunoprecipitation; ETS, E26 transformation–specific; GC, glucocorticoid; GERP, genomic evolutionary rate profiling; GR, GC receptor; GRE, GC response element; GWAS, genome-wide association study; hMDM, monocyte-derived macrophage in humans; IP, immunoprecipitation; mBMDM, bone marrow–derived macrophage in mouse; nGRE, negative GR-binding element; RT-qPCR, quantitative RT-PCR; SNP, single-nucleotide polymorphism; TSS, transcription start site; UCSC, University of California, Santa Cruz.

negative GR-binding elements (nGRE) (30, 31), which are distinct from the consensus GRE. Aside from their ability to repress the actions of proinflammatory stimuli, GC alone act directly on macrophages, producing changes in cell survival, proliferation, morphology, and phagocytosis (32–35). In other cellular systems, GR binds DNA mainly at *cis*-regulatory elements (36) and alters chromatin organization (37–39).

We sought evidence of the evolutionary pressure on GC actions by comparing the responses of human and mouse macrophages. Only limited expression data for macrophages responding to GC have been generated previously (40–42). We confirmed that the majority of genes with a significant shift in expression in response to GC are upregulated (36), but few target genes were shared between the two species. GR binding sites were enriched near to inducible genes in both species, and species-specific binding was associated with species-specific upregulation of genes in the same genomic region. However, these species-specific sites do not appear to be experiencing a selective pressure, and the only selection we could detect was for the preservation of the small set of GR binding sites that were shared between humans and mice.

Materials and Methods

Ethics

Procedures involving human volunteers were approved by the South East Scotland National Health Service Research Ethics Committee. All volunteers gave informed consent. Animals were cared for and managed within the Roslin Institute's guidelines for animal safety and welfare.

Cell culture

Eight- to 10-wk male wild-type C57BL/6 mice were culled by cervical dislocation. Bone marrow was flushed from hind limbs and then cultured in RPMI 1640 supplemented with penicillin/streptomycin, Glutamax (Invitrogen), and 10% FCS for 7 d in the presence of human rCSF-1 at 10^4 U/ml. Human peripheral blood monocytes were isolated from blood samples by Ficoll gradient separation of buffy coats, followed by MACS CD14+ve selection (Miltenyi Biotec). They were then cultured as above for 7 d before being treated as indicated with 100 nM dexamethasone (Sigma-Aldrich) or ethanol vehicle.

RNA extraction and processing

RNA was prepared using RNeasy column-based extraction with on-column DNase treatment (Qiagen). RNA quality was checked using a 2100 Bioanalyzer (Agilent). For quantitative RT-PCR (RT-qPCR), cDNA was prepared using SuperscriptIII (Invitrogen). Relative expression was determined using SyBR Green on a LightCycler480 (Roche) and compared with GAPDH as a reference. Primer sequences are given in Supplemental Table 1G. For expression microarrays, RNA was prepared using standard Affymetrix protocols and applied to the HT-MG430PM (mouse), or HT-U33plusPM (human) chip by Edinburgh Genomics.

Chromatin immunoprecipitation

Abs used for chromatin immunoprecipitation of mouse GR were BuGR2 1 μg/10^6 cells (ThermoFisher/Pierce) and normal rabbit IgG sc-2025 (Santa Cruz). For human GR chromatin immunoprecipitation (ChIP) we used Sigma-Aldrich Imprint anti-GR, 1 μg/10^6 cells, and mouse IgG.

To prepare Ab-bound beads, 20 μl protein A Dynabeads (Invitrogen) per immunoprecipitation (IP) were washed once and then diluted to 200 μl in block solution (1× PBS, 0.5% BSA, and 2 μl 0.1 M PMSF). Ab was added and rotated for 3 h at 4˚C.

Cells were washed gently once with PBS; cross-linked in tissue culture plates with 1% formaldehyde/RPMI 1640 at room temperature for 10 min (mouse) or 7.5 min (human); and then quenched with 0.125 M glycine. Cells were detached by scraping in PBS and then spun down (400 × *g*, 5 min, 4˚C), resuspended, and counted. For bone marrow–derived macrophages in mouse (mBMDM), 10^6 cells per IP were then lysed for 15 min on ice in 1% SDS, 10 mM EDTA, and 50 mM Tris-HCl (pH 8.1) supplemented with protease inhibitors (Calbiochem), 1 mM DTT, and 0.2 mM PMSF (Sigma-Aldrich). The solution was diluted in IP dilution buffer (0.1% Triton X-100, 2 mM EDTA, 150 mM NaCl, 20 mM Tris-HCl [pH 8.1]) and sonicated using a Soniprep 150 to produce an average fragment size 300–500 bp. Chromatin was spun for 10 min at 10,000 × *g*, 4˚C, and then supplemented with 20% Triton X-100 1% and BSA (Sigma-Aldrich) to 50 μg/ml. Input aliquots were removed and stored at −20˚C. Chromatin was then added to the Ab-bound protein A Dynabeads (Life Technologies) and rotated overnight at 4˚C. Beads were washed three times for 10 min each in 1–1% IP dilution buffer, 2–1% Triton X-100/0.1% Na-deoxycholate/0.1% SDS, 50 mM HEPES (pH 7.9), 500 mM NaCl, 1 mM EDTA and 3–0.5% Na-deoxycholate/0.5% Nonidet P-40, 20 mM Tris-HCl (pH 8), 1 mM EDTA, and 250 mM LiCl. Chromatin was extracted at 37˚C for 15 min on a vibrating platform in 100 ml extraction buffer (0.1 M $NaHCO_3$, 1% SDS). To reverse cross-links, samples were supplemented to 300 mM with NaCl, treated with 20 mg RNase A (Roche), and then incubated for ∼8 h at 65˚C. Proteinase K (40 μg; Genaxxon) was added, and samples were incubated at 55˚C for 1 h. DNA was purified using the QIAquick PCR purification kit (Qiagen). Real-time quantitative PCR analysis to determined percent input bound at known GR target loci was carried out on a LightCycler 480 System using SYBR Green Master Mix (Roche). Primers used are presented in Supplemental Table 1G. For sequencing ChIP DNA was prepared and amplified using Illumina adapters and Tru-Seq multiplex primers and then sequenced using a HiSeq2500 by Edinburgh Genomics.

For monocyte-derived macrophages in humans (hMDM), the same protocol was followed with the following differences. Due to constraints on cell number for sequencing, material was prepared from four volunteers, treated, fixed for 7.5 min, and lysed, as above. Consistency of the assay was assessed by biological replicates of ChIP quantitative PCR for a known GR target in the *FKBP5* locus (Supplemental Fig. 2A). Chromatin was sonicated to a fragment size of 400–600 bp, and the chromatin was pooled, to give 25 × 10^6 cells in total. This was split into three for the IP step and recombined at extraction. DNA was then isolated as above, split into three aliquots, and blunt ended with Klenow (Roche), polynucleotide kinase (New England Biolabs), and T4 DNA polymerase (Roche). An overhanging A base was added using Klenow (-exo) (New England Biolabs) and Illumina adapters ligated overnight at 16˚C with T4 DNA ligase (New England Biolabs). The IP samples were recombined after ligation and then split again into seven aliquots. Libraries were amplified from each of these aliquots using Illumina Tru-seq multiplex primers and Phusion high-fidelity DNA polymerase (New England Biolabs), and the resulting material was pooled and sequenced by Edinburgh Genomics on a Hiseq-2500.

Data analysis

Expression data. Analysis was performed using R/Bioconductor packages arrayQualityMetrics, affy, and limma (43–45). Expression values were generated using rma. Further exploratory expression analysis used unlogged expression values prefiltered for low expressed probe sets as input for the graphical correlation-based tool Biolayout Express^{3D} (46). A range of correlation coefficients and Markov Cluster Algorithm values was used to determine an optimal graph structure from which clusters of genes were then read. Clusters were then manually curated to remove artifacts. Genes from these lists were selected across a range of fold changes for analysis by RT-qPCR and a threshold drawn at log2 fold change = 1, where all tested genes were confirmed (Supplemental Fig. 1A, 1B). To limit loss of genes with extreme profiles—and hence less likely to cluster—genes reaching log2 fold change >1.5 using a conventional analysis by log fold change were also retained if the corresponding expression profile was consistent with a response across all replicates. Orthologs were identified using the Human Genome Organisation Gene Nomenclature Committee Comparison of Orthology Predictions tool (47).

Promoter analysis

Promoters were defined as −300, +100 bp of the transcription start sites (TSS) described by the FANTOM5 Consortium (48). Where multiple TSS are known, any overlaps were concatenated. Average sequence conservation scores (phastCons) for promoter regions were extracted, and enriched motifs were identified using HOMER (49).

Comparison to genome-wide association study results and inflammatory genes

The genome-wide association study (GWAS) catalog (50) (http://www.genome.gov/gwastudies/) was manually edited to retain only hits with association to inflammatory/immune conditions (Supplemental Table IH, 1408 unique single-nucleotide polymorphisms [SNPs]). The intersection of reported genes was assessed by fold change above a background distribution generated using permutation (100,000) of random gene sets. Significance of the difference was assessed using Pearson's χ^2 test. The intersection of risk SNPs and promoters was ascertained using BEDtools (51).

Functional annotation

Lists of functional terms from multiple publically available databases were generated using HOMER (49), filtered using a threshold of −log p value 6.5, and then manually curated to remove duplicate terms.

ChIP sequencing

Sequencing quality was assessed with FastQC (http://www.bioinformatics.babraham.ac.uk/projects/fastqc), and sequence from adapters was removed using trimmomatic (52). Paired end reads were aligned to mm9 or hg19 by Bowtie2 (53) using default options (-D 15 -R 2 -L 22 -i S,1,1.15). Downstream analysis was performed using HOMER (49), including creation of bedGraph files for visualization, peak calling, and annotation. Peaks were called by comparison with the sequenced input sample for each experiment as a measure of background. For the mBMDM data after confirming congruence (86% peak overlap), data from two independent replicates were combined. Publically available sequencing data for comparisons were accessed via the National Center for Biotechnology Information Gene Expression Omnibus for Uhlenhaut et al. (40) (GSE31796) and Ostuni et al. (54) (GSE38379).

We compared the number of observed intersections of our GR bound sites with sites of PU.1 binding, H3K4me1, H3K4me3, H3K27ac, and FAIRE-seq reported in unstimulated mBMDM (54) to the median intersection that occurred in 1000 genome-permuted GR peak locations. Counts of intersections for all marks were generated using HOMER (mergePeaks −cobound −d given).

To compare the locations of GC-regulated genes with GR peaks, we calculated the proportion of peaks within a given genomic interval from the TSS of a regulated gene (Fig. 3A, 3B). We calculated the enrichment of GR peaks near to regulated genes as the ratio of the proportion of regulated genes near to a GR peak to the proportion of unregulated genes with a GR peak within the same genomic interval. The significance of both these results was estimated by comparing them to the 95% confidence interval of 1000 replicates of genome-permuted GR peak locations.

We compared peaks between species using liftOver provided by University of California, Santa Cruz (UCSC) to get the coordinates of those peaks falling within syntenic blocks. Peaks with >1-bp overlap were assigned as shared. Insertions and deletions were called by comparison with dog (CanFam2), horse (EquCab2), cow (BosTau6), and pig (SuScr3) genomes. If the sequence underlying a peak could be aligned to at least one of these species, the peak was defined as being deleted; if not, then it was called an insertion. Human GR sites were assigned as deletions in along the mouse lineage (Fig. 2). Where multiple orthologs were present, this analysis was run "all to all."

The role of species-specific GR binding was assessed by calculating the proportion of genes with GR binding within 1 Mb that were upregulated to the proportion of all genes that were upregulated. These ratios were calculated separately for each combination of shared, mouse-specific, and human-specific GR peaks and upregulated genes (Fig. 4). Significance of the difference between mouse- and human-specific binding was assessed using Pearson's χ^2.

To compare the enrichment of motifs in shared versus aligned nonbound peaks, we performed motif finding using HOMER as above, using the nonbound as background.

Genomic evolutionary rate profiling (GERP) scores for the locations of bound GR motifs in both humans and mice were extracted from the UCSC genome browser. These scores have been calculated by running the GERP++ algorithm on the 36-way mammalian genome alignments (55).

Data access

Microarray and sequencing data presented in this paper have been submitted to the National Center for Biotechnology Information Gene Expression Omnibus (http://www.ncbi.nlm.nih.gov/geo/), accession GSE61881. Publically available sequencing data for comparisons were accessed via the National Center for Biotechnology Information Gene Expression Omnibus for Uhlenhaut et al. (40) (GSE31796) and Ostuni et al. (54) (GSE38379).

Results

Glucocorticoid-induced gene expression in macrophages

The response to GC was determined by gene expression profiling, using the most commonly used models of macrophage biology, mBMDM, and hMDM, both cultivated in vitro using the macrophage growth factor, CSF1 (56–58), as used in a previous comparison of the response to LPS (8).

To identify both initial direct targets and downstream secondary consequences, gene expression was measured at six time points over 24 h following treatment with dexamethasone. After filtering for low expressed and low variance probes, lists of regulated genes were confirmed by RT-qPCR (see *Materials and Methods* and Supplemental Fig. 1A, 1B) to produce a high confidence set. For mBMDM there were 160 induced and 50 repressed genes over the full 24-h time series. In the hMDM, 225 genes were induced and 125 repressed (Fig. 1A, 1B; full lists are presented in Supplemental Tables 1A, 1B). In both species, induced genes responded more quickly than repressed genes: in mBMDM, 10, 32, and 62% within 1, 2, and 4 h, respectively, compared with the repressed gene set (0, 4, and 14% at the same time points). The equivalent figures for hMDM were 11, 30, and 70% induced within 1, 2, and 4 h, respectively (2, 14, and 47% for the repressed set at the same time points).

For mBMDM and hMDM, the robust induced gene set included several known GR targets [e.g., Dusp1, Tsc22d3, Fkbp5 (40), and Per1 (36)]. As expected from earlier studies of mBMDM (59), both repressed gene lists contained urokinase plasminogen activator (Plau) (60). Because Plau is a target of sustained MAPK signaling (60), its repression may be an indirect consequence of the induction of the MAPK inhibitor Dusp1. In mBMDM, eight annotated transcription factors were among the induced gene set, including four (Fos, Hivep2, Klf4, Ncoa5) that were induced within 2 h and that could contribute to the downstream regulatory cascade. Similarly, 10 transcription factors were induced and 2 repressed within 2 h in hMDM (Supplemental Table IC). Functional annotation revealed a number of terms shared by the induced sets in both species, including stimulus response, immune/wounding response, and regulation of transcription (Supplemental Fig. 1C). The terms nuclear processes, apoptosis, and development were enriched in the early-induced set; cell surface immune response, phagocytosis, migration, and cytoskeleton were found among the late responders in mBMDM. Functional annotation of induced genes from hMDM revealed terms absent from the mouse data set, including the following: adipogenesis, FOXO and insulin signaling, and MAPK cascade. The terms immune pathways, IL-10 production, NF-κB, TNF, NOD-like receptor, and rheumatoid arthritis were enriched in the hMDM-repressed set (Supplemental Fig. 1C).

Genes regulated by GC in human macrophages are candidates for involvement in inflammatory and metabolic disease. Indeed, among GC-regulated genes in hMDM there was a 3.7-fold enrichment of genes reported to have a genetic association with an inflammatory condition or metabolic disease ($n = 48$, χ^2, $p = 1.1 \times 10^{-5}$; Supplemental Tables 1D, 1H) in the GWAS catalog (50). In mBMDM, only three of these genes were upregulated following GC treatment (Fos, Mertk, and Tlr7).

GC gene induction in hMDM differs from mBMDM

A total of 228 mouse orthologs for the 225 GC-induced hMDM genes and 131 orthologs for 125 repressed genes was identified (see *Materials and Methods*). The reciprocal analysis found 157 human orthologs of 160 mBMDM-induced and 55 orthologs of 50 mBMDM-repressed genes. From among this set of robustly regulated genes, 33 induced and 3 repressed genes were shared by the two species (Supplemental Table IE), a small but significant overlap ($p = 4 \times 10^{-15}$, cumulative binomial probability). The magnitude of expression change between genes upregulated in both species compared with the complete set of upregulated genes was only marginally different, being greater for the mouse genes (1.4-fold enrichment, Wilcoxon rank sum, $p = 9 \times 10^{-4}$).

Promoters of genes induced by GC in hMDM and mBMDM are conserved

Despite their discordant regulation between the species, and in contrast to the situation for the response of macrophages to LPS (8), the promoter regions of GC-inducible genes were conserved (Fig. 1C–E). The genes that had a shared response did not have significantly higher promoter conservation ($p = 0.166$ and $p = 0.3117$ compared with

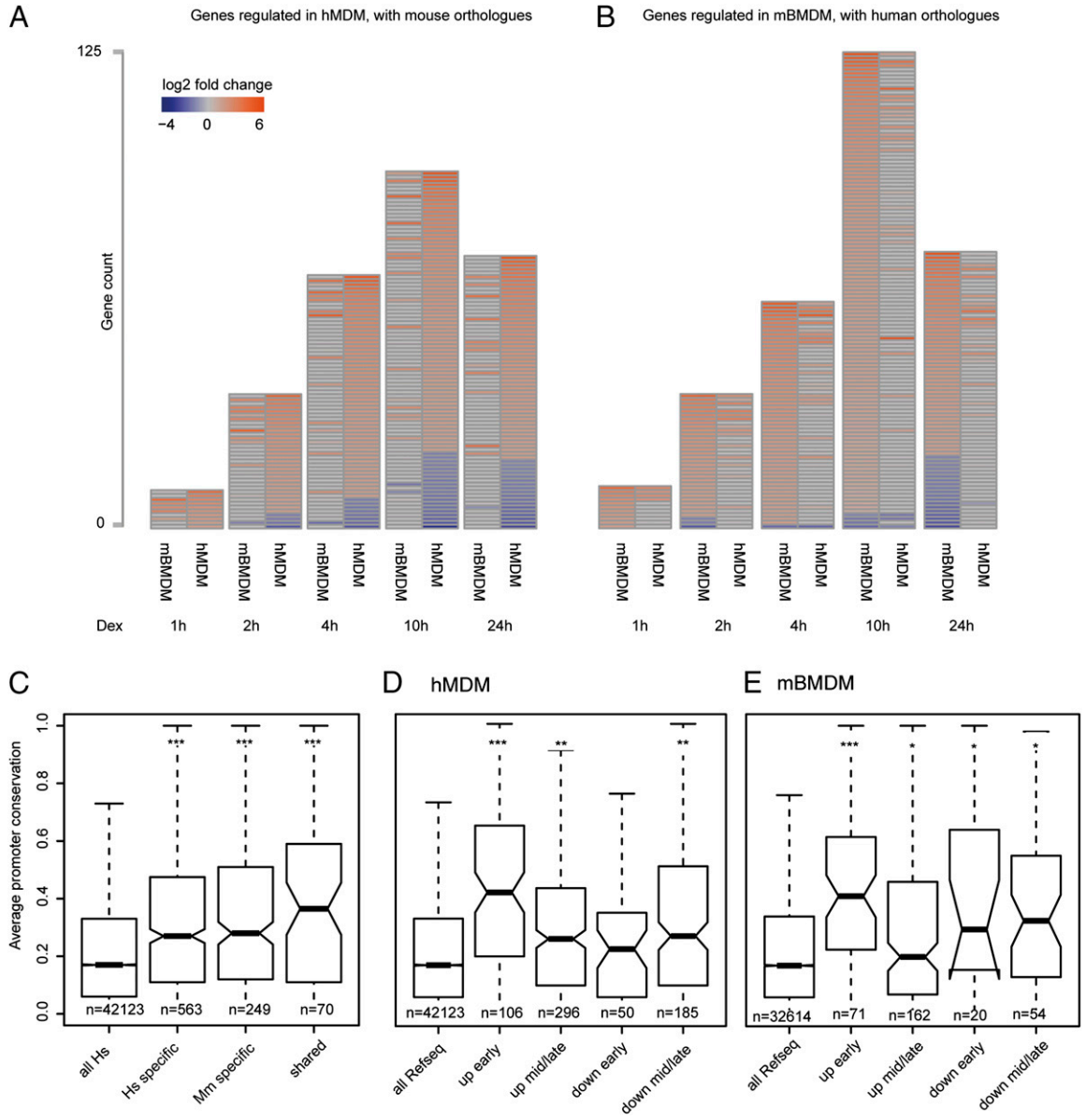

FIGURE 1. The expression response of macrophages to dexamethasone is divergent despite target gene promoter sequence conservation. (**A**) For each time point studied, heatmaps of genes regulated by 100 nM dexamethasone in hMDM alongside the orthologous genes from mouse and their expression values in mBMDM with height proportional to the number of genes changing (red = induced, blue = repressed). (**B**) The inverse analysis to that in (A) showing genes regulated in mBMDM by 100 nM dexamethasone alongside their human orthologs. (**C**) Box plots showing average sequence conservation scores (phastCons) of promoters for (all Hs) all human genes, genes responding only in either hMDM (Hs specific) or mBMDM (Mm specific) and genes with a shared expression response (shared). (**D** and **E**), as in (C), but for all genes regulated by GC in (D) mBMDM and (E) hMDM, categorized by response and kinetics. All Refseq promoters are shown as a measure of background (***$p < 1 \times 10^{-10}$, **$p < 1 \times 10^{-4}$, *$p < 0.05$, Wilcoxon rank sum; n = number of promoters; median = horizontal bar, whiskers = 1.5× interquartile range, statistical comparisons are made to background).

human specific and mouse specific, respectively; Wilcoxon rank sum) (Fig. 1C). In each species, promoters of genes that were induced the most rapidly to GC were more highly conserved than those with a slower response or than for genes whose expression was repressed in response to GC (Fig. 1D, 1E).

Analysis of the promoters (−300 bp, +100 bp of the TSS defined previously by capped analysis of gene expression analysis) (48) of GC-regulated genes for transcription factor-binding motifs provided no evidence of enrichment for GREs, and few motifs were even marginally enriched in the induced gene sets (analysis not shown).

GR binding occurs at canonical GRE sites in distal enhancers

To identify the sites involved in the GC response in the two species, chromatin immunoprecipitation for GR and sequencing (ChIP-seq) was performed 2 h after dexamethasone treatment in both mBMDM and hMDM. Representative UCSC browser tracks for GR binding in mBMDM and hMDM are shown in Fig. 2A and 2C.

There were 488 high-confidence GR-binding peaks in chromatin from mBMDM, most (474) of which were induced by dexamethasone. These peaks lie away from promoters, in intergenic regions and introns (Supplemental Fig. 2B). Based upon de novo motif finding, the majority (78%) of the GR peaks contained a motif, or motifs, closely resembling the GRE within ±25 bp of the peak center. This figure rises to 86% when considering a region ± 100 bp from the peak center (Fig. 2B). There were no matches under the GR peaks for the nGRE [CTCC(n)0-2GGAGA, where (n)0-2 indicates flexibility in spacing] (30). A more permissive search revealed 59 of 488 peaks containing a weak match for

nGRE. Of these, only 4 have a repressed gene within 1 Mb (Plau, Egr2, Rgs2, Cy2s1), one of which has a prominent canonical GRE-containing peak at 74 kb (Rgs2).

In hMDM treated with dexamethasone, 484 high-confidence GR peaks were detected (Fig. 2C). As in the mouse data, these were remote from promoters in noncoding regions of the genome (Supplemental Fig. 2B) and were highly enriched for a motif closely matching the consensus GRE (52% within ±25 bp, 62% within ± 100 bp) (Fig. 2D, Supplemental Table 2B), but not for the nGRE. None of the inflammation-associated SNPs from the GWAS catalog identified above (Supplemental Table IG) directly overlap with GR-bound peaks in hMDM, although two lie within 350 bp (rs10499197, near TNFAIP3 linked to systemic lupus erythematosus and systemic sclerosis and rs12466022, linked to multiple sclerosis).

Inducible transcription factors often bind to regions that are already in open chromatin. The GR peaks in mBMDM were clearly associated with sites marked by various enhancer-associated histone marks in unstimulated cells (Supplemental Fig. 2C). Overall, 462 of 488 (94%) of our sites overlap with one or more enhancer marks (Supplemental Fig. 2C), and individual marks also showed enrichments above genome-wide expectations (H3K27ac [70.3%, 24.5-fold enriched, $p < 2.2 \times 10^{-16}$], H3K4me1 [90.4%, 18.4-fold enriched, $p < 2.2 \times 10^{-16}$]) and open chromatin (43.4%, 53.9-fold enriched, $p < 2.2 \times 10^{-16}$). The E26 transformation-specific (ETS) factor PU.1 is a master regulator of macrophage transcription, and other stimulus-induced transcription factors have been shown to bind at enhancers marked by PU.1 in activated macrophages (49, 61). The sites recruiting GR after dexamethasone treatment also show significant overlap with PU.1 binding sites in unstimulated mBMDM (72.3%, 32.1-fold enriched, $p < 2.2 \times 10^{-16}$ Pearson's χ^2; Supplemental Fig. 1C). Overall, a close match to the PU.1 consensus motif was found in 36% of GR-bound sites in mBMDM (Fig. 2B, $p = 1 \times 10^{-79}$), and 76% had an ETS motif. Similarly, 34% of GR peaks in treated hMDM had a PU.1 motif (Fig. 2D, $p = 1 \times 10^{-36}$) and 62% an ETS factor-binding motif. The GRE and ETS sites were closely spaced

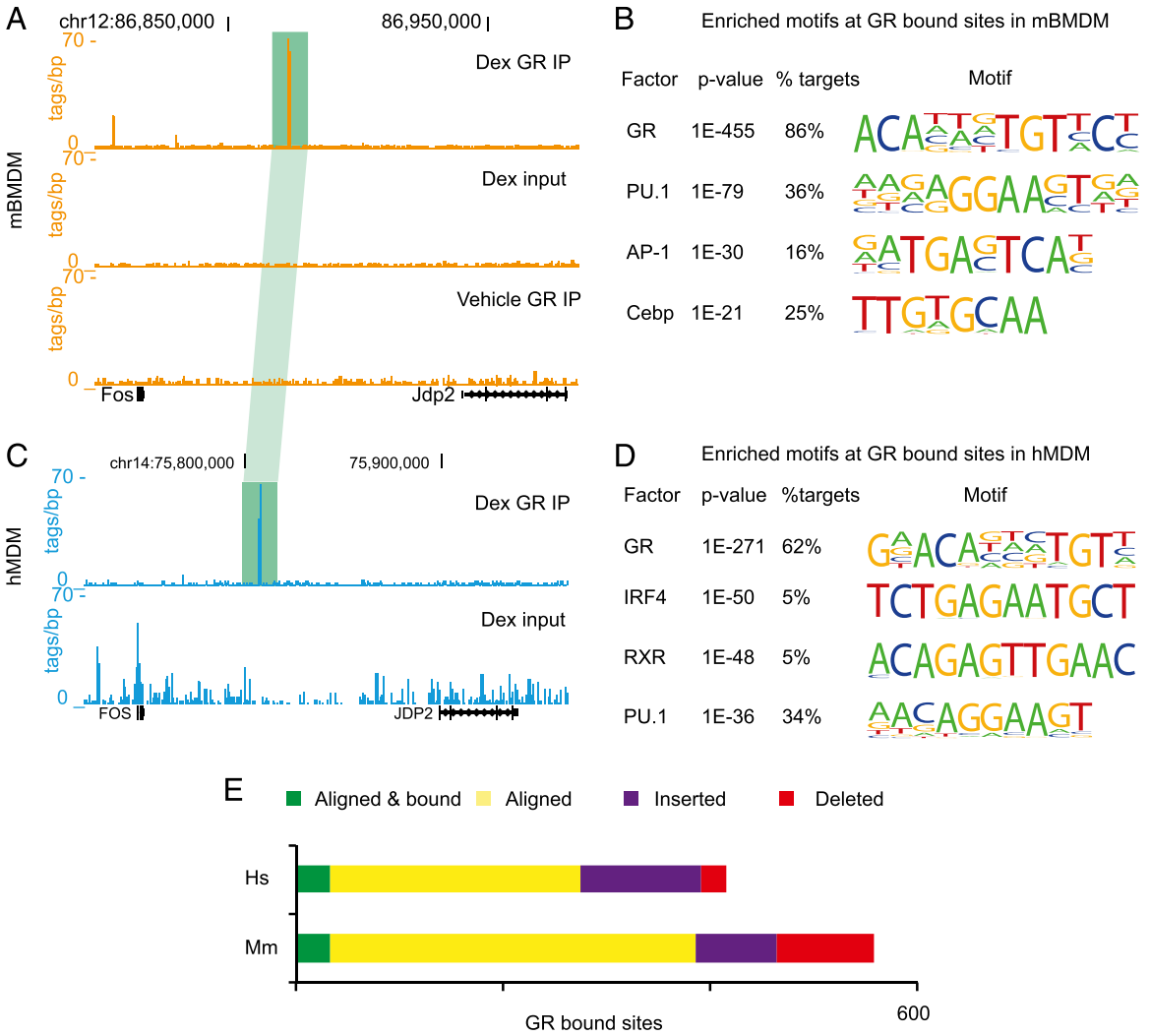

FIGURE 2. GR binding in mBMDM and hMDM occurs at sites with the canonical GRE. (**A**) ChIP-seq data tracks from the UCSC browser for the Fos–Jdp2 region, for GR binding in mBMDM. Data from ChIP with anti-GR Abs after treatment with 100 nM dexamethasone for 2 h (Dex GR IP), input material (Dex input), and immunoprecipitated material from a vehicle-treated control (Vehicle GR IP) are shown. (**C**) As in (A), but for FOS–JDP2 in hMDM. Vehicle GR IP data were not generated in hMDM due to constraints on available cell numbers. A GR-bound site that aligns between mBMDM and hDMD is highlighted in green. Alignments are to mm9 and hg19 versions of the mouse and human genomes, respectively. (**B** and **D**) Enriched motifs found de novo within GR-bound sites in mBMDM (B) and hMDM (D). (**E**) Evolutionary outcomes for GR peaks in human. Aligned sites where the orthologous region is bound by GR in mice are shown in green and in yellow if the site is not bound by GR in mice. Sites that could not be aligned are defined as either insertions (purple) or deletions (red) by comparison with dog (CanFam2), horse (EquCab2), cow (BosTau6), and pig (SuScr3) genomes (see *Materials and Methods*). Human GR sites were assigned as deletions in the mouse lineage.

(average of 40 bp between the motifs in mice and 43 bp in humans), suggestive of cooperativity between ETS factors and GR binding. Aside from PU.1, there was little similarity in other transcription factor motifs enriched around the GR peaks in the two species. For the mouse, other enriched motifs include those that can bind Cepb, AP-1, c-Jun, and Runx1 (Fig. 2B). For the hMDM data set, IFN regulatory factor 4 and RXR sites were the most significantly enriched (Fig. 2D).

GR binding differs in hMDM and mBMDM

The majority of GR-bound sites can be aligned between humans and mice (n = 274 [56.6%] and 354 [79.2%] in humans and mice, respectively), but only a minority of these (n = 32) are bound by GR in both (Fig. 2E, Supplemental Table 1F). There was no difference between the rate of turnover of GR binding in evolution at these sites in humans and mice (χ^2, $p = 0.18$). Sites that could not be aligned between humans and mice were defined as de novo insertions if they could not be aligned to any of several outgroup species, or deletions if they could be (see *Materials and Methods*). As previously reported (62), there was an increased rate of deletions along the mouse lineage (3.8-fold, χ^2, $p = 2.6 \times 10^{-11}$) and a smaller, but significant, 1.6-fold increased rate of insertions along the human lineage (χ^2, $p = 2.0 \times 10^{-3}$). There have been several reports that transposable elements are the source of species-specific sequences (14, 63). Indeed, transposable elements were the source of almost all inserted GR-binding sequence (96.6 and 75.5% in humans and mice, respectively), which represent 1.8- and 1.4-fold enrichments (χ^2, $p < 7.6 \times 10^{-3}$) over the deleted sequences in humans and mice, respectively.

GR binding is associated with induced genes in both human and mouse macrophages, but the target loci are not conserved

There was a clear association between GR-binding peaks and the loci encoding GC-induced genes in both human and mouse macrophages. This enrichment was greatest at 10 kb from the TSS, but still marginally detectable at 1 Mb in both species (Fig. 3). In A549 cells, GR has been reported to be bound closer to induced genes than to repressed genes (36), whereas in our macrophage data, there was no detectable relationship between GR-binding peaks and repressed genes (Fig. 3).

The expression response to GC was stronger where there were multiple GR peaks within 200 kb of the TSS of an induced gene than if there was only a single site (mBMDM, 1.7-fold median $\log_2$ fold change, $p = 0.0018$; hMDM, 1.4-fold median $\log_2$ fold change, $p = 0.031$, Wilcoxon rank sum). Early (<2 h) induction was not associated with greater proximity to a GR peak (Wilcoxon rank sum, $p = 0.20$ and $p = 0.16$, for humans and mice, respectively).

As stated above, among the set of GR-bound sites from hMDM and mBMDM that can be assigned to regions of conserved DNA, only a minority (n = 32) were clearly conserved in binding (Supplemental Table IF). Sixteen of the conserved GR sites are adjacent to genes that were induced in both species and that encode known regulators of the inflammatory response (e.g., DUSP1, FKBP5, MAP3K6, TSC22D3, FOS [Fig. 2A, 2C], KLF4). Even at these conserved loci, GR binding differed: a previously described proximal peak at the DUSP1/Dusp1 locus was retained (64), but the strongest binding site was not shared (Fig. 4A). Overall, genes that were induced in both species were enriched for having GR bound within 1 Mb—but not necessarily at orthologous positions—in both species (4.0-fold enrichment, χ^2, $p = 2.9 \times 10^{-7}$; Fig. 4A).

The more common pattern was for GR binding at regulated loci to be divergent between the species; for example, the GR peak upstream of F13a1, a component of the coagulation cascade, is mouse specific (Fig. 4C, expanded view in Supplemental Fig. 2D). Genes like F13a1 that responded to GC only in mouse were 2.0-fold enriched over human-specific genes for GR binding within 1 Mb in the mouse (χ^2, $p = 0.0011$; Fig. 4D). Similarly, human-specific GR binding was enriched adjacent to human-specific GC-regulated genes. For example, ADORA3, which has a known role in driving the human macrophage phenotype (65), has an intronic GR peak that is not present in mouse. As for the mouse, there was an overall 1.7-fold enrichment for a human-specific GR

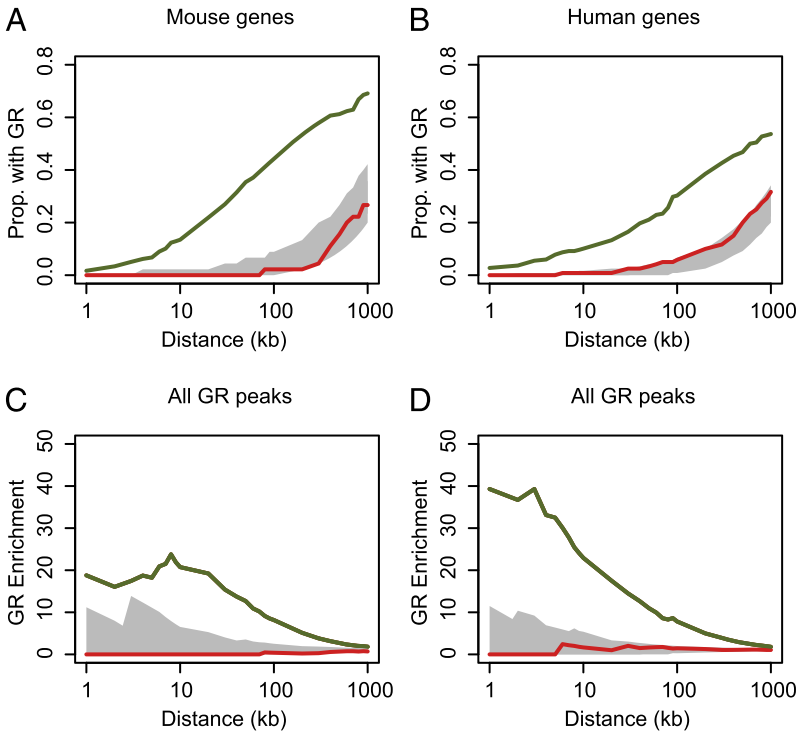

FIGURE 3. Induced genes are associated with GR binding. (**A** and **B**) The proportion of GR ChIP peaks with induced (green line) or repressed (red line) gene promoters within a given genomic distance for (A) mBMDM and (B) hMDM. The 95% confidence intervals from matched genome-permuted distributions of GR peaks are shown in gray. (**C** and **D**) Enrichment of the proportion of induced (green line) gene promoters with a GR peak within a given interval versus the proportion of induced genes without a GR peak (red line) within that interval for (C) mBMDM and (D) hMDM. No enrichment is seen for repressed genes (shown in red). The 95% confidence interval from a genome-permuted distribution of GR peaks is shown in gray.

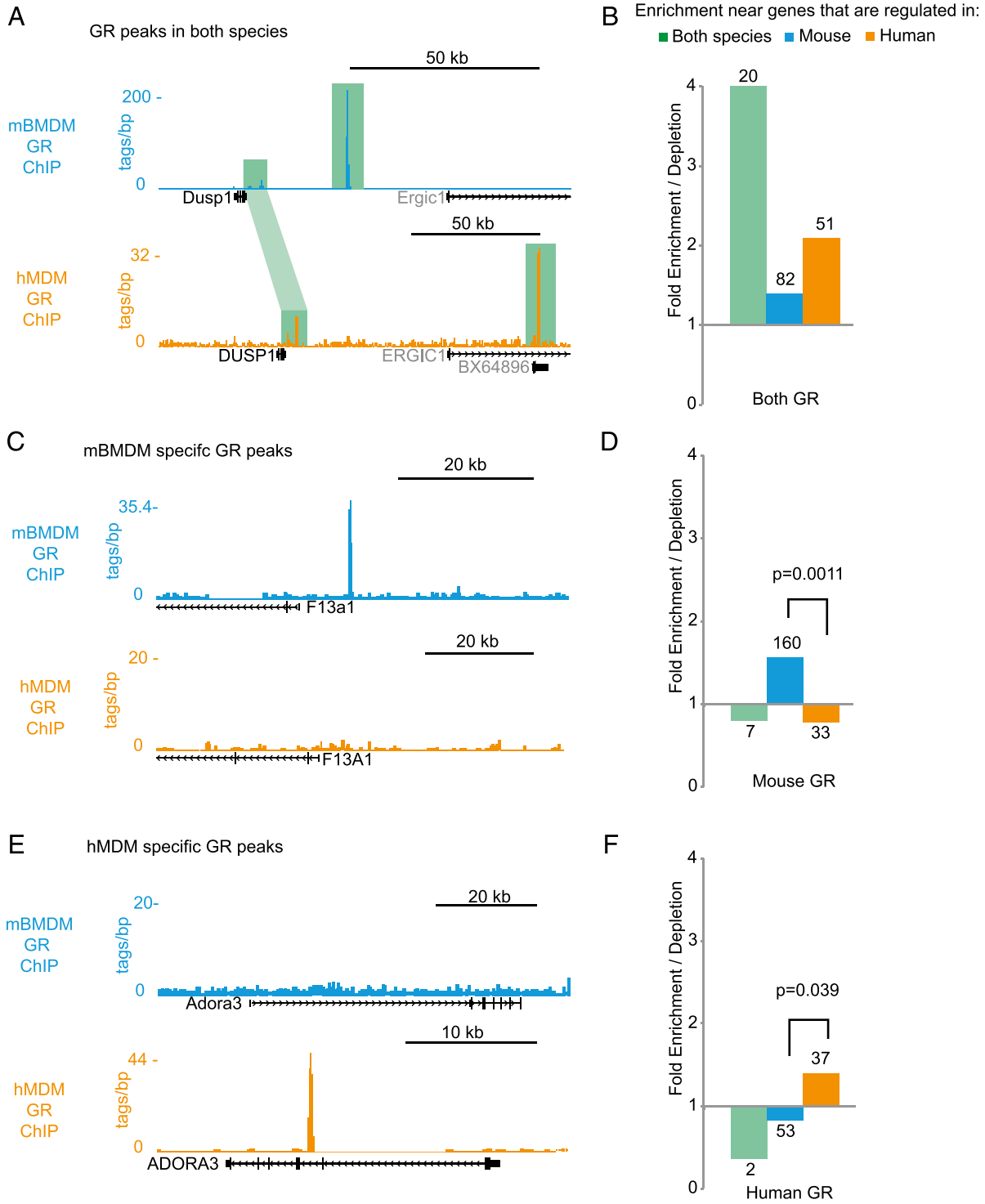

FIGURE 4. GR binding sites are minimally conserved between mice and humans, and this is linked to the divergent transcriptional response to GC. (**A**) GR ChIP-seq data from mBMDM (orange) and hMDM (cyan) showing conserved GR binding (green highlight) at a locus (DUSP1/Dusp1) whose expression is rapidly induced by GC in both mouse and human macrophages. GR-bound sites aligned between species are linked by light green highlight: the most prominent sites are bound in only one species. (**B**) Enrichment/Depletion for mouse/human shared GR binding within 1 Mb for GC-responsive genes that are shared between mice and humans (green), mouse specific (cyan) and human specific (orange). Numbers give raw counts for each category. (**C**) As in (A), but showing mouse-specific GR binding at F13a1/F13A1, which is induced in mBMDM, but not hMDM. (**D**) As for (B), but for mouse-specific GR binding sites. The χ^2 p value for the difference between mouse- and human-specific sites is given. (**E**) As in (A), but showing human-specific GR binding at ADORA3/Adora3, which is induced in hMDM, but not mBMDM. (**F**) As for (D), but for human-specific GR binding sites. Expanded windows for F13A1 and Adora3 are shown in Supplemental Fig. 1D.

peak within 1 Mb genes that were specifically upregulated in human macrophages (χ^2, p = 0.034; Fig. 4E, 4F, expanded view in Supplemental Fig. 2D). These data highlight the strong correlation between divergent GR binding and divergent gene expression response to dexamethasone across species (Figs. 1, 2), and the shared enrichment for GR binding in the vicinity of genes that were induced in both species (Fig. 3). We conclude that the turnover of GR binding sites between humans and mice is the primary driver of the divergent transcriptional response to GC.

Most of the species-specific GR sites are in genomic regions that can be aligned between mice and humans (Fig. 2E), suggesting that the changes that cause motif loss occurred as a result of nucleotide substitutions and deletions, rather than insertion or deletion of sequence. Loss of GR binding was associated with loss of the GRE motif. Among aligning sequence, there was significant enrichment for the GRE motif in the subset that is bound in both species compared with those that are species specific (Fig. 5). This is also true for PU.1, although less strongly, reflecting the lower enrichment for this motif in the baseline data set. Consistent with the loss of GR binding, there was depletion for the GRE motif in locations that were not bound by GR, even when the orthologous location in the opposite species was bound (Supplemental Fig. 3A, 3B). There was some enrichment for PU.1 in human sequence orthologous to mouse-specific sites, which suggests there may be some residual regulatory function in macrophages at these sites.

The turnover of the GRE motif at species-specific GR peaks could be driven by a selective pressure on the immune response to modulate host–pathogen interactions (8, 23). Evolutionary constraint was detectable around the shared sites in each species (Fig. 5C, 5D), extending to ~100 bp beyond the motif (Supplemental Fig. 3C, 3D). This implies that purifying selection has acted to preserve this motif between humans and mice. As predicted by the degeneracy of the GRE motif, evidence of selection was reduced in the center of the motif. However, within the species-specific GR binding sites, there was no signature consistent with substantial selection across the motif (Fig. 5C, 5D). Indeed, there was some slight constraint at the non-degenerate sites in the motif. This suggests that turnover of the GRE motif at individual loci is driven by nucleotide substitutions at approximately the genome-wide mutation rate and not by positive selection driving the gain or loss of new binding sites (Fig. 4).

Discussion

This study shows that the divergence of the transcriptional response to GC in mouse and human macrophages is associated with evolutionary turnover of candidate enhancers. These enhancers contain canonical inverted repeat GRE and are bound by GR in glucocorticoid-treated macrophages. Although GC have commonly been studied as repressors of inflammatory gene expression, the data indicate that, in the context studied in this work, GC act on macrophages primarily as inducers of gene expression when measured at the level of stable mRNA. The induced targets are largely distinct between humans and mice (Fig. 1). This adds to the weight of evidence that caution must be exercised when translating mouse findings to humans (8, 21, 22).

Repressed genes have been shown to lie further from GR-bound sites than induced genes at candidate loci (66) and in previously published ChIP-seq data from A549 lung epithelial cancer cell line (36). Based upon genome-wide comparison, the genes repressed after GC treatment in macrophages had no significant genomic association with direct GR–DNA binding in either species (Fig. 3), nor was there any support for the existence of nGRE (30, 31) in either mouse or human GR ChIP-seq data sets. Lower binding affinity and faster turnover time could compromise their detection under the conditions we employed. Alternatively, there may be context-dependent use of different types of regulatory element. For example, the nGRE may only be relevant in macrophages when GR acts to suppress inflammatory gene induction (40), rather than in the basal CSF1-dependent state we have examined. The GC-responsive GR elements we identified were often associated with binding motifs for the macrophage master transcription factor PU.1. Therefore, as for other transcription factors downstream of extracellular signaling (49, 54), the GR-binding landscape is shaped by enhancer elements already occupied by PU.1.

Evolutionary conservation has long been used to identify candidate functional regions of the genome (67). A very small subset of GC-induced genes and nearby GR-bound sites fits this pattern. These genes are enriched for a number of shared functional annotations, such as stimulus response and immune/wounding response (Supplemental Fig. 1C), whereas the shared GR sites were found near to induced genes in both species (Figs. 3, 4). The shared GR-bound sites were subject to evolutionary constraint of the GR-binding motif (Fig. 5), suggesting they have been exposed

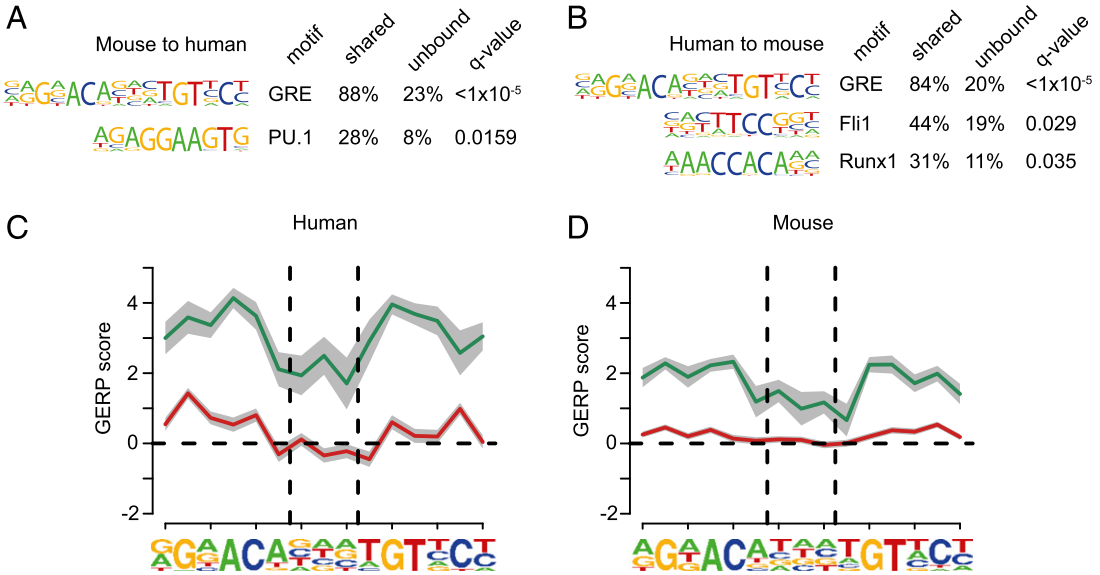

FIGURE 5. Conserved GR binding is linked to conservation of the GRE. (**A**) Motif enrichment for the sites bound by GR in mBMDM that aligned and were also bound in hMDM, using as background the mouse sites that could be aligned to human, but were not bound in hMDM (q values shown, Benjamini-Hochberg). (**B**) Analogous to (A), but for hMDM sites bound in mBMDM versus sites that could be aligned, but were not bound in mBMDM. (**C**) Mean per base constraint scores calculated using GERP (55) across the GRE in shared (green) and species-specific (red) peaks found in hMDM, where the gray bars represent the SEM. Vertical dashed lines delineate the center NNN for the GRE, as derived de novo from our hMDM data. (**D**) Analogous to (C) for GR-bound peaks and GRE motif found in mBMDM.

to purifying selection to maintain their function in humans and mice.

The large majority of the GR-bound sites were not conserved between mice and humans. The level of divergence we found between GR binding sites and motifs between human and mouse macrophages is greater than that previously reported for a set of liver-specific transcription factors, in which 20–30% of sites were conserved between primates and rodents (13). Although our data set is limited to one factor and motif, it would appear that GC-responsive elements are even more divergent than the sites identified in liver, which would be consistent with previous observations for high divergence in long-range regulatory elements active in immune tissues (7).

The gain or loss of these GR-bound sites is largely due to nucleotide substitutions, rather than insertion or deletion of sequence (Fig. 2), as previously reported for a set of liver enhancers (17). These substitutions cause gain or loss of the canonical GRE as well as partner motifs such as PU.1 (Fig. 5). These turnover events had a biological consequence: they were clearly associated with species differences in transcriptional regulation (Fig. 4C–F). The macrophage subtypes studied in this work are not directly comparable, and there are known species differences in the response to CSF1, which produces a proatherogenic signal in human macrophages, but not in mice (58). However, the association with sequence turnover strongly suggests that the divergent expression response to GC is unrelated to the differences in the regulatory network of different macrophage populations (68). Sequence variation also underlies the divergent response of macrophages to LPS, but in that case it was attributable to promoter sequence variation (8).

There was no clear evidence for selection at species-specific GR sites, which show functional turnover between humans and mice (Fig. 5C, 5D). Some of these sites may be under lineage-specific selection, in the same way that LPS-responsive genes are shared by large animals (humans and pigs) but radically different in rodents (8, 69). Such variation would not be detectable with the available genomic sequence data. Alternatively, the associated species-specific inducible genes may not have any function in the feedback regulation of innate immunity. Some of the species-specific GR-bound peaks might have arisen by chance within regions that favor open chromatin in macrophages, and bind GR solely as a consequence of high transcription factor concentrations in the nucleus (70).

An interesting avenue for further research will be the physiological consequences of the functional genomic changes that we have found. We cannot say from our study how the genomic changes are related to the substantial phenotypic differences between species, or how much effect change at any one locus might have. One way to begin to address this would be, at a locus that normally only responds to GC in humans, to insert the sequence of the human GRE at the equivalent position in the mouse genome and compare the response.

The general principles of the macrophage response to GC are strongly conserved between mice and humans, but the specific loci involved have diverged considerably. As previously reported (13, 71), we have shown large-scale turnover of candidate enhancers and have extended this work by demonstrating that these turnover events impact on inducible gene expression. Surprisingly, given the divergence at *cis*-regulatory sequence associated with immunity (7) and the potential drive of host–pathogen interactions on macrophages, we could not detect evidence of positive selection at species-specific GR-bound sites. Conserved elements, in contrast, showed clear evidence of selection to preserve their characteristic motifs. Despite much interest in the turnover of enhancers (72), the traditional approach of identifying regulatory elements through deep evolutionary conservation may still be most useful in identifying those sites associated with conserved gene regulation.

Acknowledgments

We thank R. Illingworth (Medical Research Council Human Genetics Unit) for assistance with optimizing ChIP-seq assays and Edinburgh Genomics for running microarrays and sequencing samples.

Disclosures

The authors have no financial conflicts of interest.

References

1. Ponting, C. P. 2008. The functional repertoires of metazoan genomes. *Nat. Rev. Genet.* 9: 689–698.
2. King, M. C., and A. C. Wilson. 1975. Evolution at two levels in humans and chimpanzees. *Science* 188: 107–116.
3. Wittkopp, P. J., and G. Kalay. 2012. Cis-regulatory elements: molecular mechanisms and evolutionary processes underlying divergence. *Nat. Rev. Genet.* 13: 59–69.
4. McCarroll, S. A., C. T. Murphy, S. Zou, S. D. Pletcher, C. S. Chin, Y. N. Jan, C. Kenyon, C. I. Bargmann, and H. Li. 2004. Comparing genomic expression patterns across species identifies shared transcriptional profile in aging. *Nat. Genet.* 36: 197–204.
5. Khaitovich, P., I. Hellmann, W. Enard, K. Nowick, M. Leinweber, H. Franz, G. Weiss, M. Lachmann, and S. Pääbo. 2005. Parallel patterns of evolution in the genomes and transcriptomes of humans and chimpanzees. *Science* 309: 1850–1854.
6. Fairfax, B. P., P. Humburg, S. Makino, V. Naranbhai, D. Wong, E. Lau, L. Jostins, K. Plant, R. Andrews, C. McGee, and J. C. Knight. 2014. Innate immune activity conditions the effect of regulatory variants upon monocyte gene expression. *Science* 343: 1246949.
7. Yue, F., Y. Cheng, A. Breschi, J. Vierstra, W. Wu, T. Ryba, R. Sandstrom, Z. Ma, C. Davis, B. D. Pope, et al. 2014. A comparative encyclopedia of DNA elements in the mouse genome. *Nature* 515: 355–364.
8. Schroder, K., K. M. Irvine, M. S. Taylor, N. J. Bokil, K.-A. Le Cao, K.-A. Masterman, L. I. Labzin, C. A. Semple, R. Kapetanovic, L. Fairbairn, et al. 2012. Conservation and divergence in Toll-like receptor 4-regulated gene expression in primary human versus mouse macrophages. *Proc. Natl. Acad. Sci. USA* 109: E944–E953.
9. Odom, D. T., R. D. Dowell, E. S. Jacobsen, W. Gordon, T. W. Danford, K. D. MacIsaac, P. A. Rolfe, C. M. Conboy, D. K. Gifford, and E. Fraenkel. 2007. Tissue-specific transcriptional regulation has diverged significantly between human and mouse. *Nat. Genet.* 39: 730–732.
10. Bulger, M., and M. Groudine. 2011. Functional and mechanistic diversity of distal transcription enhancers. *Cell* 144: 327–339.
11. Pennacchio, L. A., N. Ahituv, A. M. Moses, S. Prabhakar, M. A. Nobrega, M. Shoukry, S. Minovitsky, I. Dubchak, A. Holt, K. D. Lewis, et al. 2006. In vivo enhancer analysis of human conserved non-coding sequences. *Nature* 444: 499–502.
12. Visel, A., J. Bristow, and L. A. Pennacchio. 2007. Enhancer identification through comparative genomics. *Semin. Cell Dev. Biol.* 18: 140–152.
13. Ballester, B., A. Medina-Rivera, D. Schmidt, M. Gonzàlez-Porta, M. Carlucci, X. Chen, K. Chessman, A. J. Faure, A. P. Funnell, A. Goncalves, et al. 2014. Multi-species, multi-transcription factor binding highlights conserved control of tissue-specific biological pathways. *eLife* 3: e02626.
14. Vierstra, J., E. Rynes, R. Sandstrom, M. Zhang, T. Canfield, R. S. Hansen, S. Stehling-Sun, P. J. Sabo, R. Byron, R. Humbert, et al. 2014. Mouse regulatory DNA landscapes reveal global principles of cis-regulatory evolution. *Science* 346: 1007–1012.
15. Stergachis, A. B., S. Neph, R. Sandstrom, E. Haugen, A. P. Reynolds, M. Zhang, R. Byron, T. Canfield, S. Stelhing-Sun, K. Lee, et al. 2014. Conservation of trans-acting circuitry during mammalian regulatory evolution. *Nature* 515: 365–370.
16. Stefflova, K., D. Thybert, M. D. Wilson, I. Streeter, J. Aleksic, P. Karagianni, A. Brazma, D. J. Adams, I. Talianidis, J. C. Marioni, et al. 2013. Cooperativity and rapid evolution of cobound transcription factors in closely related mammals. *Cell* 154: 530–540.
17. Villar, D., C. Berthelot, S. Aldridge, T. F. Rayner, M. Lukk, M. Pignatelli, T. J. Park, R. Deaville, J. T. Erichsen, A. J. Jasinska, et al. 2015. Enhancer evolution across 20 mammalian species. *Cell* 160: 554–566.
18. Kunarso, G., N.-Y. Chia, J. Jeyakani, C. Hwang, X. Lu, Y.-S. Chan, H.-H. Ng, and G. Bourque. 2010. Transposable elements have rewired the core regulatory network of human embryonic stem cells. *Nat. Genet.* 42: 631–634.
19. Biggin, M. D. 2011. Animal transcription networks as highly connected, quantitative continua. *Dev. Cell* 21: 611–626.
20. Bradley, R. K., X. Y. Li, C. Trapnell, S. Davidson, L. Pachter, H. C. Chu, L. A. Tonkin, M. D. Biggin, and M. B. Eisen. 2010. Binding site turnover produces pervasive quantitative changes in transcription factor binding between closely related Drosophila species. *PLoS Biol.* 8: e1000343.
21. Mestas, J., and C. C. W. Hughes. 2004. Of mice and not men: differences between mouse and human immunology. *J. Immunol.* 172: 2731–2738.

22. Seok, J., H. S. Warren, A. G. Cuenca, M. N. Mindrinos, H. V. Baker, W. Xu, D. R. Richards, G. P. McDonald-Smith, H. Gao, L. Hennessy, et al. 2013. Genomic responses in mouse models poorly mimic human inflammatory diseases. *Proc. Natl. Acad. Sci. USA* 110: 3507–3512.
23. Wells, C. A., T. Ravasi, G. J. Faulkner, P. Carninci, Y. Okazaki, Y. Hayashizaki, M. Sweet, B. J. Wainwright, and D. A. Hume. 2003. Genetic control of the innate immune response. *BMC Immunol.* 4: 5.
24. Chinwalla, A. T., L. L. Cook, K. D. Delehaunty, G. A, Fewell, L. A. Fulton, R. S. Fulton, T. A. Graves, L. W. Hillier, E. R. Mardis, J. D. McPherson, et al. 2002. Initial sequencing and comparative analysis of the mouse genome. *Nature* 420: 520–562.
25. Nicolaides, N. C., E. Kyratzi, A. Lamprokostopoulou, G. P. Chrousos, and E. Charmandari. 2015. Stress, the stress system and the role of glucocorticoids. *Neuroimmunomodulation* 22: 6–19.
26. Fardet, L., I. Petersen, and I. Nazareth. 2011. Prevalence of long-term oral glucocorticoid prescriptions in the UK over the past 20 years. *Rheumatology* 50: 1982–1990.
27. Nixon, M., R. Andrew, and K. E. Chapman. 2013. It takes two to tango: dimerisation of glucocorticoid receptor and its anti-inflammatory functions. *Steroids* 78: 59–68.
28. Ratman, D., W. Vanden Berghe, L. Dejager, C. Libert, J. Tavernier, I. M. Beck, and K. De Bosscher. 2013. How glucocorticoid receptors modulate the activity of other transcription factors: a scope beyond tethering. *Mol. Cell. Endocrinol.* 380: 41–54.
29. Rogatsky, I., H. F. Luecke, D. C. Leitman, and K. R. Yamamoto. 2002. Alternate surfaces of transcriptional coregulator GRIP1 function in different glucocorticoid receptor activation and repression contexts. *Proc. Natl. Acad. Sci. USA* 99: 16701–16706.
30. Surjit, M., K. P. Ganti, A. Mukherji, T. Ye, G. Hua, D. Metzger, M. Li, and P. Chambon. 2011. Widespread negative response elements mediate direct repression by agonist-liganded glucocorticoid receptor. *Cell* 145: 224–241.
31. Hudson, W. H., C. Youn, and E. A. Ortlund. 2013. The structural basis of direct glucocorticoid-mediated transrepression. *Nat. Struct. Mol. Biol.* 20: 53–58.
32. Ehrchen, J., L. Steinmüller, K. Barczyk, K. Tenbrock, W. Nacken, M. Eisenacher, U. Nordhues, C. Sorg, C. Sunderkötter, and J. Roth. 2007. Glucocorticoids induce differentiation of a specifically activated, anti-inflammatory subtype of human monocytes. *Blood* 109: 1265–1274.
33. Varga, G., J. Ehrchen, A. Tsianakas, K. Tenbrock, A. Rattenholl, S. Seeliger, M. Mack, J. Roth, and C. Sunderkoetter. 2008. Glucocorticoids induce an activated, anti-inflammatory monocyte subset in mice that resembles myeloid-derived suppressor cells. *J. Leukoc. Biol.* 84: 644–650.
34. Galon, J., D. Franchimont, N. Hiroi, G. Frey, A. Boettner, M. Ehrhart-Bornstein, J. J. O'Shea, G. P. Chrousos, and S. R. Bornstein. 2002. Gene profiling reveals unknown enhancing and suppressive actions of glucocorticoids on immune cells. *FASEB J.* 16: 61–71.
35. van de Garde, M. D. B., F. O. Martinez, B. N. Melgert, M. N. Hylkema, R. E. Jonkers, and J. Hamann. 2014. Chronic exposure to glucocorticoids shapes gene expression and modulates innate and adaptive activation pathways in macrophages with distinct changes in leukocyte attraction. *J. Immunol.* 192: 1196–1208.
36. Reddy, T. E., F. Pauli, R. O. Sprouse, N. F. Neff, K. M. Newberry, M. J. Garabedian, and R. M. Myers. 2009. Genomic determination of the glucocorticoid response reveals unexpected mechanisms of gene regulation. *Genome Res.* 19: 2163–2171.
37. John, S., P. J. Sabo, T. A. Johnson, M.-H. Sung, S. C. Biddie, S. L. Lightman, T. C. Voss, S. R. Davis, P. S. Meltzer, J. A. Stamatoyannopoulos, and G. L. Hager. 2008. Interaction of the glucocorticoid receptor with the chromatin landscape. *Mol. Cell* 29: 611–624.
38. John, S., P. J. Sabo, R. E. Thurman, M.-H. Sung, S. C. Biddie, T. A. Johnson, G. L. Hager, and J. A. Stamatoyannopoulos. 2011. Chromatin accessibility predetermines glucocorticoid receptor binding patterns. *Nat. Genet.* 43: 264–268.
39. Trotter, K. W., H.-Y. Fan, M. L. Ivey, R. E. Kingston, and T. K. Archer. 2008. The HSA domain of BRG1 mediates critical interactions required for glucocorticoid receptor-dependent transcriptional activation in vivo. *Mol. Cell. Biol.* 28: 1413–1426.
40. Uhlenhaut, N. H., G. D. Barish, R. T. Yu, M. Downes, M. Karunasiri, C. Liddle, P. Schwalie, N. Hübner, and R. M. Evans. 2013. Insights into negative regulation by the glucocorticoid receptor from genome-wide profiling of inflammatory cistromes. *Mol. Cell* 49: 158–171.
41. Chinenov, Y., M. Coppo, R. Gupte, M. A. Sacta, and I. Rogatsky. 2014. Glucocorticoid receptor coordinates transcription factor-dominated regulatory network in macrophages. *BMC Genomics* 15: 656.
42. Xue, J., S. V. Schmidt, J. Sander, A. Draffehn, W. Krebs, I. Quester, D. De Nardo, T. D. Gohel, M. Emde, L. Schmidleithner, et al. 2014. Transcriptome-based network analysis reveals a spectrum model of human macrophage activation. *Immunity* 40: 274–288.
43. Smyth, G. K. 2005. Limma: linear models for microarray data. In *Bioinformatics and Computational Biology Solutions Using {R} and Bioconductor.* R. Gentleman, V. Carey, S. Dudoit, R. Irizarry, and W. Huber, eds. Springer, New York, p. 397–420.
44. Gautier, L., L. Cope, B. M. Bolstad, and R. A. Irizarry. 2004. affy–analysis of Affymetrix GeneChip data at the probe level. *Bioinformatics* 20: 307–315.
45. Kauffmann, A., R. Gentleman, and W. Huber. 2009. arrayQualityMetrics–a bioconductor package for quality assessment of microarray data. *Bioinformatics* 25: 415–416.
46. Theocharidis, A., S. van Dongen, A. J. Enright, and T. C. Freeman. 2009. Network visualization and analysis of gene expression data using BioLayout Express(3D). *Nat. Protoc.* 4: 1535–1550.
47. Gray, K. A., L. C. Daugherty, S. M. Gordon, R. L. Seal, M. W. Wright, and E. A. Bruford. 2013. Genenames.org: the HGNC resources in 2013. *Nucleic Acids Res.* 41: D545–D552.
48. The FANTOM Consortium and the RIKEN PMI and CLST (DGT). 2014. A promoter-level mammalian expression atlas. *Nature* 507: 462–470.
49. Heinz, S., C. Benner, N. Spann, E. Bertolino, Y. C. Lin, P. Laslo, J. X. Cheng, C. Murre, H. Singh, and C. K. Glass. 2010. Simple combinations of lineage-determining transcription factors prime cis-regulatory elements required for macrophage and B cell identities. *Mol. Cell* 38: 576–589.
50. Hindorff, L. A., P. Sethupathy, H. A. Junkins, E. M. Ramos, J. P. Mehta, F. S. Collins, and T. A. Manolio. 2009. Potential etiologic and functional implications of genome-wide association loci for human diseases and traits. *Proc. Natl. Acad. Sci. USA* 106: 9362–9367.
51. Quinlan, A. R., and I. M. Hall. 2010. BEDTools: a flexible suite of utilities for comparing genomic features. *Bioinformatics* 26: 841–842.
52. Bolger, A. M., M. Lohse, and B. Usadel. 2014. Trimmomatic: a flexible trimmer for Illumina sequence data. *Bioinformatics* 30: 2114–2120.
53. Langmead, B., and S. L. Salzberg. 2012. Fast gapped-read alignment with Bowtie 2. *Nat. Methods* 9: 357–359.
54. Ostuni, R., V. Piccolo, I. Barozzi, S. Polletti, A. Termanini, S. Bonifacio, A. Curina, E. Prosperini, S. Ghisletti, and G. Natoli. 2013. Latent enhancers activated by stimulation in differentiated cells. *Cell* 152: 157–171.
55. Davydov, E. V., D. L. Goode, M. Sirota, G. M. Cooper, A. Sidow, and S. Batzoglou. 2010. Identifying a high fraction of the human genome to be under selective constraint using GERP++. *PLOS Comput. Biol.* 6: e1001025.
56. Hume, D. A., W. Allan, J. Golder, R. W. Stephens, W. F. Doe, and H. S. Warren. 1985. Preparation and characterization of human bone marrow-derived macrophages. *J. Leukoc. Biol.* 38: 541–552.
57. Ingersoll, M. A., R. Spanbroek, C. Lottaz, E. L. Gautier, M. Frankenberger, R. Hoffmann, R. Lang, M. Haniffa, M. Collin, F. Tacke, et al. 2010. Comparison of gene expression profiles between human and mouse monocyte subsets. *Blood* 115: e10–e19.
58. Irvine, K. M., M. R. Andrews, M. A. Fernandez-Rojo, K. Schroder, C. J. Burns, S. Su, A. F. Wilks, R. G. Parton, D. A. Hume, and M. J. Sweet. 2009. Colony-stimulating factor-1 (CSF-1) delivers a proatherogenic signal to human macrophages. *J. Leukoc. Biol.* 85: 278–288.
59. Hume, D. A., and S. Gordon. 1984. The correlation between plasminogen activator activity and thymidine incorporation in mouse bone marrow-derived macrophages: opposing actions of colony-stimulating factor, phorbol myristate acetate, dexamethasone and prostaglandin E. *Exp. Cell Res.* 150: 347–355.
60. Stacey, K. J., L. F. Fowles, M. S. Colman, M. C. Ostrowski, and D. A. Hume. 1995. Regulation of urokinase-type plasminogen activator gene transcription by macrophage colony-stimulating factor. *Mol. Cell. Biol.* 15: 3430–3441.
61. Ghisletti, S., I. Barozzi, F. Mietton, S. Polletti, F. De Santa, E. Venturini, L. Gregory, L. Lonie, A. Chew, C.-L. Wei, et al. 2010. Identification and characterization of enhancers controlling the inflammatory gene expression program in macrophages. *Immunity* 32: 317–328.
62. Laurie, S., M. Toll-Riera, N. Radó-Trilla, and M. M. Albà. 2012. Sequence shortening in the rodent ancestor. *Genome Res.* 22: 478–485.
63. Bejerano, G., C. B. Lowe, N. Ahituv, B. King, A. Siepel, S. R. Salama, E. M. Rubin, W. J. Kent, and D. Haussler. 2006. A distal enhancer and an ultraconserved exon are derived from a novel retroposon. *Nature* 441: 87–90.
64. Tchen, C. R., J. R. S. Martins, N. Paktiawal, R. Perelli, J. Saklatvala, and A. R. Clark. 2010. Glucocorticoid regulation of mouse and human dual specificity phosphatase 1 (DUSP1) genes: unusual cis-acting elements and unexpected evolutionary divergence. *J. Biol. Chem.* 285: 2642–2652.
65. Barczyk, K., J. Ehrchen, K. Tenbrock, M. Ahlmann, J. Kneidl, D. Viemann, and J. Roth. 2010. Glucocorticoids promote survival of anti-inflammatory macrophages via stimulation of adenosine receptor A3. *Blood* 116: 446–455.
66. So, A. Y.-L., S. B. Cooper, B. J. Feldman, M. Manuchehri, and K. R. Yamamoto. 2008. Conservation analysis predicts in vivo occupancy of glucocorticoid receptor-binding sequences at glucocorticoid-induced genes. *Proc. Natl. Acad. Sci. USA* 105: 5745–5749.
67. Haeussler, M., and J. S. Joly. 2011. When needles look like hay: how to find tissue-specific enhancers in model organism genomes. *Dev. Biol.* 350: 239–254.
68. Lavin, Y., D. Winter, R. Blecher-Gonen, E. David, H. Keren-Shaul, M. Merad, S. Jung, and I. Amit. 2014. Tissue-resident macrophage enhancer landscapes are shaped by the local microenvironment. *Cell* 159: 1312–1326.
69. Kapetanovic, R., L. Fairbairn, D. Beraldi, D. P. Sester, A. L. Archibald, C. K. Tuggle, and D. A. Hume. 2012. Pig bone marrow-derived macrophages resemble human macrophages in their response to bacterial lipopolysaccharide. *J. Immunol.* 188: 3382–3394.
70. MacArthur, S., X.-Y. Li, J. Li, J. B. Brown, H. C. Chu, L. Zeng, B. P. Grondona, A. Hechmer, L. Simirenko, S. V. E. Keränen, et al. 2009. Developmental roles of 21 Drosophila transcription factors are determined by quantitative differences in binding to an overlapping set of thousands of genomic regions. *Genome Biol.* 10: R80.
71. Schmidt, D., M. D. Wilson, B. Ballester, P. C. Schwalie, G. D. Brown, A. Marshall, C. Kutter, S. Watt, C. P. Martinez-Jimenez, S. Mackay, et al. 2010. Five-vertebrate ChIP-seq reveals the evolutionary dynamics of transcription factor binding. *Science* 328: 1036–1040.
72. Villar, D., P. Flicek, and D. T. Odom. 2014. Evolution of transcription factor binding in metazoans: mechanisms and functional implications. *Nat. Rev. Genet.* 15: 221–233.